

Airflow in a Domestic Kitchen Oven measured by Particle Image Velocimetry

C.J.T.Spence¹, N.A.Buchmann¹, M.C.Jermy¹

¹Department of Mechanical Engineering
University of Canterbury, Private Bag 4800, Christchurch, New Zealand

Abstract

Particle Image Velocimetry (PIV) was used to map the internal airflow of a domestic kitchen oven. Oven cooking performance is dependant on the airflow within the cavity. Previous flow measurement techniques such as hot wire anemometry and pitot probes are very time consuming and prone to error in the hot recirculating flow in an oven. The oven cavity, a commercially available mid-range oven, was modified for optical access. The PIV system consisted of a CCD camera, light sheet illumination from a pulsed Nd:YAG laser, and propanediol droplets and hollow glass spheres with a Stokes number of less than 0.055. Experiments were conducted in an empty oven at room temperature and at 180°C, and at 180°C with a single cooking tray installed. Velocity fields were measured in seven adjacent, coplanar object planes each on four different planes in the oven. The velocity data was averaged to yield mean flow fields, and the seven coplanar data fields were subsequently collaged to produce a full cross-sectional velocity map for each oven plane.

In the cold and hot empty cavity a single vortex centred on the fan axis was seen, with strong radial flow. The maximum measured velocity in the cold oven was 1.8ms^{-1} , which compared well with earlier hot-wire measurements. When a tray was introduced, the single vortex was replaced by three circulatory features. Shear flow was seen on both upper and lower sides of the tray, with a lower velocity and a stagnation point on the upper side.

Introduction

In domestic electric fan ovens, cooking time and quality are dependant on the airflow in the oven. Areas of high velocity accelerate evaporation and heat transfer, hence cooking speed. Quantitative understanding of the airflow pattern within the oven cavity allows design improvements which enhance the ovens performance by ensuring constant cooking rates throughout the cavity.

Fellows "[2] noted that the typical objectives of a food cooking process are to achieve the desirable sensory qualities, colour, texture, flavour and aroma, while minimising weight loss and ensuring the destruction of microbial pathogens. The rate of evaporation is one of the most important parameters in achieving these objectives (Kirk [5]). The flow field in the oven therefore affects the local heat flux and can cause uneven cooking and surface browning.

The typical domestic electric fan oven is a roughly cuboid cavity with a centrifugal fan mounted on the back wall. The fan shrouding is minimal and the fan expels air at all points on its circumference. A circular heating element surrounding the fan is often the only source of heat, although other heating modes using roof or floor mounted elements are possible. The fan serves to circulate the air in an attempt to achieve an even temperature and evaporation rate for food throughout the oven. Point measurement techniques such as hot wire anemometry and Pitot-static tubes require a long time to map a 3D flow. Hot wires

encounter difficulties in flows with non-uniform temperature and Pitot-static tubes require much care to be taken over the flow direction in 3D recirculating flows. PIV has no such difficulties and can acquire data from several thousand independent measurement locations simultaneously.

Hardin and Burmeister [3] visualised the airflow in a forced convection oven with oil films, Styrofoam beads and tufts. A polycarbonate resin thermoplastic (Lexan) oven cavity was constructed and racks, inserts, motor, fan and elements fitted, although all measurements were conducted at room temperature. Results showed that airflow from the forward-curved centrifugal fan was unsymmetrical, unequal amounts of air flowed to the two sides of the oven and vortices were present in the corners of the cavity. Testing techniques employed were very time consuming and attention was confined to the flows around the fan and in the side ducts that distribute heated air from the fan to the oven cavity. Kato et al [4] used laser sheet visualisation to investigate turbulent flow inside scale models of clean rooms, which share some common features with oven flows.

Verboven et al [12] used hot-film probes (TSI-8465) to measure the time-averaged velocities in a commercial electrical plug fan forced convection oven. Their oven cavity was comparable in size to this study's oven, measuring $540 \times 720 \times 380\text{mm}$ ($W \times H \times D$). The size excluded the use of ultrasonic anemometers, which are relatively large instruments. The poor optical accessibility and cavity environment led Verboven et al to opt not to use laser-Doppler velocimetry (LDA) or fragile hot wire sensors to obtain the three-dimensional velocity field and turbulence properties. As also intended for the data from this study, Verboven et al used their experimental results to validate computational fluid dynamics calculations.

An anemometer that is sensitive at low velocity and high temperature was developed by Therdtai et al [10] to measure flow velocity in an industrial bread-baking oven. The anemometer however, was not used to measure the entire flow field in the oven, rather it was designed as an instrument that could travel through the various zones of the conveyed oven, measuring the flow velocity close to the cooking dough.

Laser flow measurement techniques have been used extensively to measure external flows and some internal flows. There were however no previous published studies conducted in closed cuboid cavities with fan forced convection found in the literature surveyed. Internal airflows, as well as often being considerably more complex than external airflows (Ostrach [8]), require enclosure modifications to accommodate optical access. Tulapurkara [11] used LDA to measure the flow velocities within a rectangular enclosure of 10mm transparent acrylic sheet with an internal volume of $600 \times 400 \times 400\text{mm}$ and circular inlet, a central partition and exit pipes of 80 and 90mm diameters, respectively. Mamun et al [6] fitted a boroscope to their cubical enclosure to enable PIV measurement of the internal flow velocities.

The oven cavity investigated in this study was a wall mounted mid-range domestic oven. The standard oven basic components included: an enamelled sheet steel cavity, with inner dimensions 480×390×390mm (W×H×D), separated from an outer shell by a layer of fibreglass insulation, a lower heating element, two upper heating elements and an oven door.

A 6-bladed centrifugal fan, driven by a fixed speed motor, is located in the centre of the oven's rear wall, rotating clockwise when viewed from the front and drawing air from the cooking cavity. The fan shroud is a plate parallel to the back of the oven enclosing the fan. It has a circular louvred vent over the entire diameter of the fan blades and the fan eye. Air is expelled at the fan's circumference, passing over a 10mm diameter circular heating element before travelling behind the shroud panel to re-enter the oven cavity via vents along the edges of the rear panel. A schematic of the modified oven is given in Figure 1 with the arrows showing the recirculating flow in and out of the cavity.

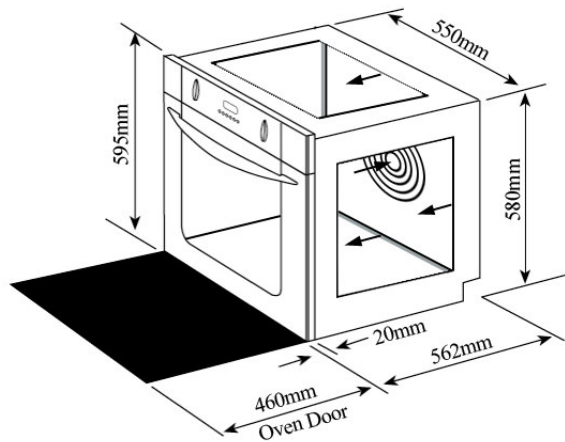


Figure 1 – Schematic of modified oven, showing flow in and out of the cavity and installed glass windows.

Previous hotwire anemometry results revealed maximum and average internal flow velocities of 1.8ms⁻¹ and 0.79ms⁻¹ respectively, however failed to build an overall flow structure within the cavity. Temperature variations within the oven cavity had also been measured using a K-type thermocouple to be approximately 8°C for a 180°C thermostatic setting.

Experimental Method

Test Conditions and Oven Modifications

Different combinations of active heating elements give a variety of available cooking modes. In this study, measurements were conducted in fan-on mode at room temperature with no heat added to the cavity. It was expected that the flow structure within the oven cavity would be similar at both room and elevated temperatures as the forced fan flow would dominate buoyancy effects. At typical cooking temperatures the Russell number (Eq. 1), which is the ratio of inertial to buoyancy forces, was 2.8. U is the velocity, L the characteristic length scale, g the acceleration due to gravity, ρ the gas density and z the vertical coordinate. For this calculation U=0.79ms⁻¹, L=0.42m (average cavity dimension) and the density was calculated at 180°C with a temperature range of 8°C.

$$Ru = \frac{U}{L \left(-\frac{g}{\rho} \frac{\partial \rho}{\partial z} \right)} \quad (1)$$

Measurements were made with both hot and cold empty cavities, and in a cavity with an oven tray(s) and racks installed. The oven cavity was modified for optical access by removing the upper and lower heating elements and adding borosilicate glass windows to the oven faces shown in Figure 1. The circular element surrounding the fan behind the rear panel was left in place. Where optical access was not required glass was covered with non-reflecting material to reduce background reflections and illumination of seeding particles outside of the light sheet. The thermal boundary conditions in hot flow experiments differed from the production oven because the fibreglass insulated sheet metal cavity faces were replaced with glass windows.

Preliminary Measurements

Flow visualisation and hot wire anemometry measurements were initially conducted within the cold, empty cavity. A flow visualisation video of the internal flow structure at room temperature was made using a reverse cyclone aerosol generator and titanium dioxide particles with an approximate diameter of 20µm and a CW light sheet.

PIV Measurements

The PIV system consisted of a pulsed 120mJ Nd:YAG laser (New Wave Solo XT 120), a 1008x1018 pix² digital CCD camera (Kodak Megaplug 1.0) with objective (Hanimax Automatic MC, focal length 28mm, f/2.8) and light sheet optics. Two convex lenses of focal lengths 170mm and 40mm were used in a reverse Galilean telescope arrangement to reduce the beam diameter exiting the laser from 5mm to 1.2mm. A negative cylindrical lens with a back focal length (BFL) of -13.16mm was used to expand this beam into a light sheet 1.5mm thick. Figure 2 illustrates the arrangement of the apparatus.

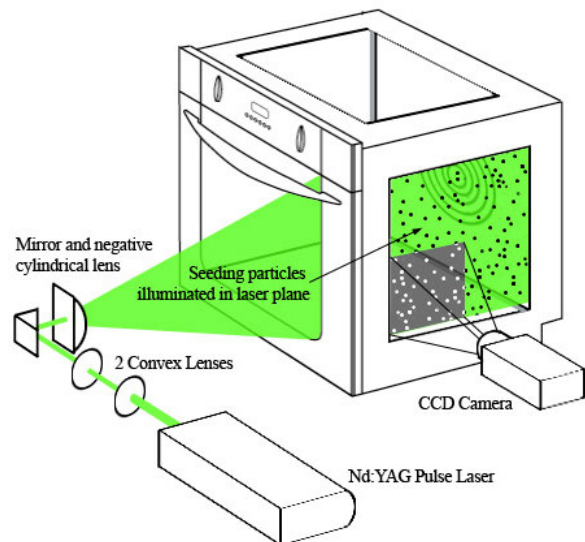


Figure 2 – Schematic of apparatus arrangement.

In the cold flow, propanediol droplets with a mean size of 6µm were used as seeding particles and were generated using multiple Wright nebulisers (Trident T1800) in parallel. In the hot flow, 10µm hollow glass spheres were introduced with a reverse cyclone seeder. For accurate PIV measurements, the Stokes number for seeding must be less than 0.1, but preferably less than 0.01 for the error induced by particle inertia to be <0.7% [1], so that the viscous forces on the particles dominates particle momentum. The maximum velocity in the cavity of 1.8ms⁻¹ was

known from previous hot wire anemometry results, giving a maximum Stokes number of 0.025 for the propanediol droplets and 0.055 for the hollow glass spheres. The seeding particles were introduced at four locations behind the cavity's rear panel at a flowrate such that an ideal seeding concentration of about 15 particles per interrogation region [7] was maintained with particle injection rate balancing particle evaporation, breakup and deposition on the walls and fan.

Successive images of the illuminated particles were recorded on $1008 \times 1018 \text{ pix}^2$ frames with time delays of 600 and 1800ms, depending on cavity location. Image pairs were taken at rates of 1 and 15Hz. After background subtraction and masking of the cavity sides, the recorded images were divided into $64 \times 64 \text{ pix}^2$ interrogation windows. Images were processed using MatPIV freeware [9]. For each region a cross-correlation of the image intensity values was calculated to determine the window average displacement and iterative refinement and displacement of the interrogation areas was performed. The displacement was calculated with sub-pixel accuracy and the interrogation regions overlapped by 50% to increase the vector density.

In order to resolve individual particles the largest allowable field of view of the $1008 \times 1018 \text{ pix}^2$ camera was $200 \times 200 \text{ mm}$. A total of 100 instantaneous velocity fields were acquired in each of seven locations on a given plane. Each set of 100 velocity fields were averaged. The seven averaged velocity fields belonging to a single plane in the oven were collaged together to obtain mean flow fields over the entire cross section of the cavity. The collaging of images used an overlap of 20mm (approx 100 pixels) between adjacent images. The velocity vectors in the overlap region were calculated using a simple unweighted average of the vectors in the contributing images.

Results and discussion

Flow visualisation experiments revealed a vortex structure, centred on the axis of the fan and rotating clockwise when viewed from the front towards the fan (Figure 3). The vortex, core was not straight and exhibited vortex precession. The rate of precessions was apparently random and the location of the core on the door (bottom edge of Fig. 3) varied with an amplitude of approximately 80mm. The vortex core diameter (cross section shown in Figure 4) was roughly constant along the length of the vortex, unlike a bathtub vortex in which the vortex tapers as it approaches the suction inlet. No recirculation zones (RZ) were observed in the corners of the oven cavity. The fan exhaust feeds into the corners adjacent the fan shroud plate, so no RZ are expected here. Air may flow from the shroud, along the walls to impinge on the corners adjacent to the door, preventing RZs from forming, or there may be RZs in these corners too weak to be observed in these images.

PIV was used to measure the flow field of three cross-sectional planes (A-C) of an empty oven cavity and a central section (D) of the cavity with an oven tray and racks installed (Figure 5). The velocity maps obtained are shown in Figures 6a-d.

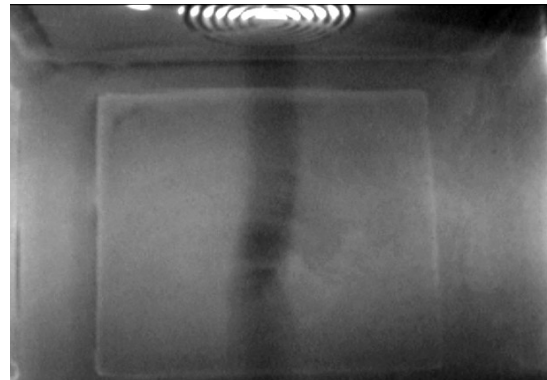


Figure 3 – Flow visualisation within the oven cavity in plan view.

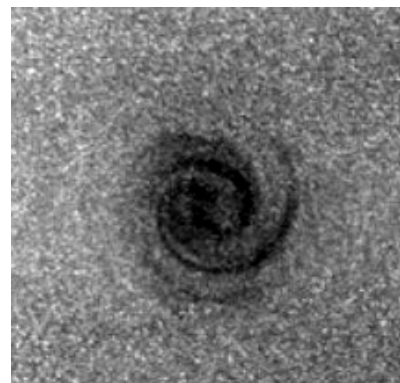


Figure 4 – Cross-section of vortex core.

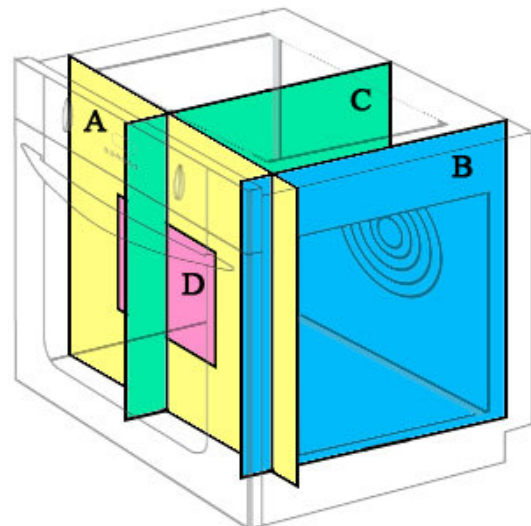


Figure 5 – Schematic showing cross-sectional planes investigated.

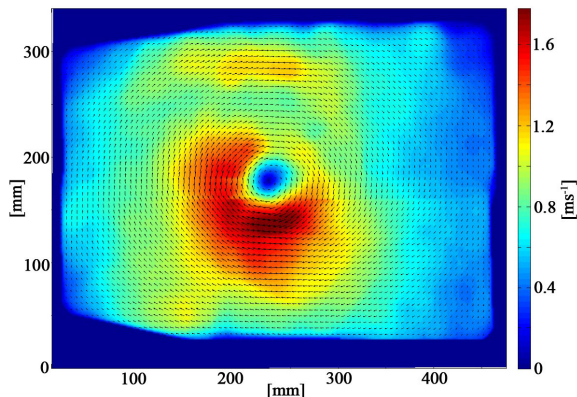


Figure 6(a) – Plane A PIV velocity map (empty oven).

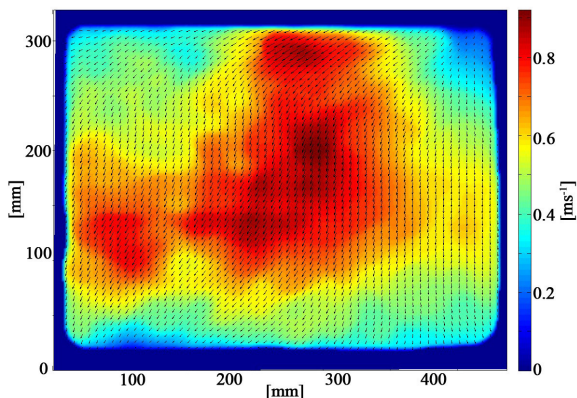


Figure 6(b) – Plane B PIV velocity map (empty oven).

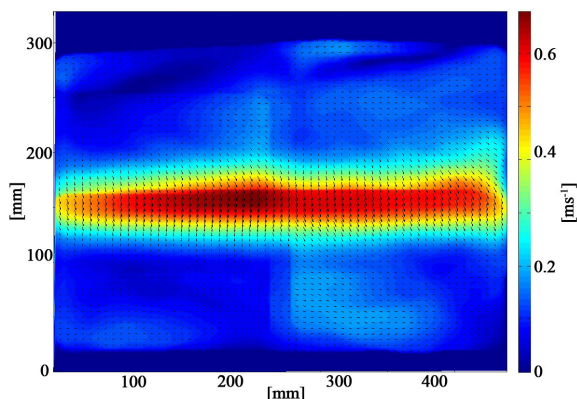


Figure 6(c) – Plane C PIV velocity map (empty oven).

PIV results quantitatively confirmed the clockwise flow structure observed in the flow visualisation. It can be seen in planes A and B (Figures 6(a) and 6(b)) that the largest velocities occurred in the centre of the oven, surrounding the vortex core. The maximum velocity measured was 1.8ms^{-1} , which agreed with previous hot wire anemometry results. A ‘c’ shaped band of high velocities is visible in Figure 7a. Although the vortex core does move during the time between the seven images sets being acquired, this does not explain this ‘c’ shaped structure. The central panel containing the vortex was acquired as one set of 100 image pairs. The ‘c’ shaped structure is real and indicates a helical structure in the flow in this near-door plane.

Earlier measurements with a handheld anemometer in the vicinity of the rear panel indicated the flow emerging from the fan shroud was not uniformly distributed, rather that the flow emerged from the left and right hand sides with a higher velocity than the flow emerging from other areas of the shroud-wall gap. These high velocity streams may persist to the door and be picked up from the door by the axial flow into the fan, creating a helical high-speed stream.

The axial flow in the vortex core is visible, moving toward the fan, in plane C (Fig. 6(c)). It was evident from planes B and C that velocities in the axial direction were smaller than the radial velocities. The axis of the fan lies in Plane C. When the plane C data was taken, the average location of the vortex was to the left of the fan axis plane (viewed from the front of the oven) i.e. behind plane C. Areas of low velocity included the corners of the oven, where no secondary vortices were observed, in contrast to [3].

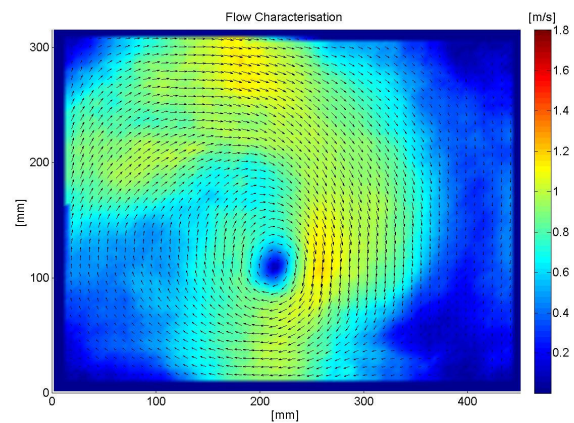


Figure 7 Plane A, empty oven at 180°C

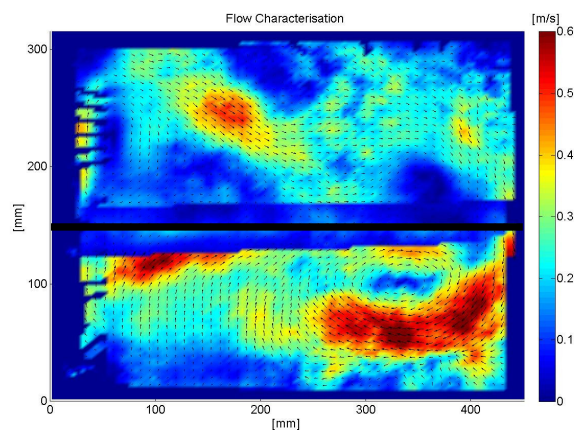


Figure 8 - Plane B PIV velocity map with a tray inserted in the centre of the cavity (bold black line), 180°C.

A velocity map of Plane A in the empty oven at 180°C is shown in Figure 7. The overall structure of the flow is similar to that in the cold, empty oven in Fig. 6(a) with the vortex core and the ‘c’ shaped band of high velocity flow surrounding it. However several of the details differ. The velocities are lower, and the vortex is offset to the left and down relative to the cold oven. This image was acquired in a different oven to that used in Fig. 6(a), with slightly different window and insulation construction and potentially a slightly different fan speed. The position of the vortex may be sensitive to the presence of minor leaks. The area

in yellow ($1.0\text{-}1.2\text{ms}^{-1}$) is similar in both hot and cold ovens, but the hot oven does not exhibit the red ($1.5\text{-}1.8\text{ms}^{-1}$) region seen in the empty oven. Measurements of the hot and cold flow in the same oven will be conducted.

Figure 8 shows the velocity map at plane B at 180°C with a flat (unlipped) cooking tray inserted halfway between the floor and ceiling. The tray carries no food. The tray lies in the low velocity band in the centre of the image. Much of this low velocity band lies in the shadow of the tray, reducing the illumination, so the velocity vectors here are meaningless. Outside this band it is clear that the nature of the flow is radically different to the empty oven. A vortex is seen beneath the tray, offset to the right. A second circulatory feature is seen above the tray also offset to the right. There is also a vortex on the left above the tray in the vicinity of the racks. These racks are the horizontal wire racks common to most fan ovens and which support the trays. There is shear flow over much of the tray surface, although there is a stagnation point on the upper side of the tray, at about 190mm from the left hand edge. The velocity near the surface of the tray is higher on the underside than on the top side. High velocities lead to high rates of heat transfer, but also of moisture loss, though evaporation is not a concern on the underside of the tray.

Conclusions

The flow field in a domestic electric fan oven has been mapped with PIV. Measurements were made at room temperature with an empty cavity and at 180°C with a cooking tray and racks installed. The flow in an empty cavity, both cold and hot, consisted of a vortex, centred on the axis of the centrifugal fan. The radial velocities were strong. When a tray was introduced, the single vortex is replaced by three circulatory features. Shear flow exists over both the upper and lower side of the tray, with a lower velocity and a stagnation point on the upper side. The velocity field is significantly non-uniform.

An understanding of oven cavity flow is necessary for the design of future ovens. Work currently in progress is addressing the differences between hot and cold flow and the effect of multiple trays.

Acknowledgments

We would like to thank Fisher and Paykel Appliances for supporting this work and Stephen Kim, Mark Fahey and Dave Hastings of F&P for illuminating discussions. We would like to acknowledge J Anderson, D Hight, CM Yiu, A Waddingham, M Wright, A Bradley and J de Tracy Gould for performing many of the measurements during their undergraduate thesis projects and

to G Harris, E Cox, D Labbe and J Chambrillon for assistance with design and construction of the equipment.

References

- [1] Dring R.P., Sizing criteria for laser anemometry particles, *Journal of fluids engineering ASME*, **104**, 1982, 15-17.
- [2] Fellows P. J., *Food processing technology principles and practice*, Woodhead Publishing Limited, Cambridge, 2000.
- [3] Hardin R. A. & Burmeister L. C., Flow visualization in a forced convection oven, in *Heat Transfer Measurements, Analysis, and Flow Visualization ASME*, New York, 1989, 133-141.
- [4] Kato S., Murakami S. & Chirfu S., Study of air flow in conventional flow type clean room by means of numerical simulation and model test, in *Proceedings of the eight International Symposium on Contamination Control*, Milan, 1986, 781-791.
- [5] Kirk D., Cooking: Understanding what happens in catering equipment, in G. Glew, *Advances in catering technology - 3*, Elsevier Applied Science, Barking, 1984, 53-63.
- [6] Mamun M. A. H., Johnson D. A. & Hollands K. G. T., PIV Measurements of the Flow Field inside an Enclosed Cubical Cavity in Natural Convection, in *12th International Symposium on Applications of Laser Techniques to Fluid Mechanics*, Lisbon, 2004.
- [7] Melling A., Tracer particles and seeding for particle image velocimetry, *Measurement Science and Technology*, **8**, 1997, 1406-1416.
- [8] Ostrach S., Natural convection in enclosures, *Journal of Heat Transfer*, **110**, 1988, 1175-1190.
- [9] Svern, J.K., MatPIV 1.6.1, <http://www.math.uio.no/~jks/matpiv/>, 2004.
- [10] Therdthai N., Zhou W. B. & Adamczak T., The development of an anemometer for industrial bread baking, *Journal of Food Engineering*, **63**, 2004, 329-334.
- [11] Tulapurkara E. G., LDA measurements inside a rectangular enclosure, Ruhr Universität, Bochum, 1995.
- [12] Verboven P., Scheerlinck N., De Baerdemaeker J. & Nicolai B. M., Computational fluid dynamics modelling and validation of the isothermal airflow in a forced convection oven, *Journal of Food Engineering*, **43**, 2000, 41-53.